

BEAM DYNAMICS IN PRESENCE OF IMPERFECTION FIELDS NEAR THE EXTRACTION ZONE OF KOLKATA SUPERCONDUCTING CYCLOTRON

J. Debnath[#], M.K. Dey, J. Pradhan, S. Paul, A. Dutta, U. Bhunia, Md. Z.A. Naser, V. Singh, A. Chakrabarti, Variable Energy Cyclotron Centre, 1/AF, Bidhan Nagar, Kolkata -700064, India

Abstract

The superconducting cyclotron at Kolkata has accelerated the ion beams up to the extraction radius producing neutrons via nuclear reactions. After that the beam extraction process has been tried exhaustively. But rigorous beam extraction trials indicate towards some kind of error field, which was not possible to balance with the trim coil operated in harmonic-coil mode. It is found that the beam is being off-centred by a large amount after crossing the resonance zone and it is not reaching the extraction radius in proper path. This paper will be emphasizing the effect of various kind of error field on the beam. However, the magnetic field is being measured again to know the exact distribution of the field.

INTRODUCTION

The superconducting cyclotron [1] at VECC is a multi-particle, variable energy machine, having bending limit of $K_b=500$ corresponding to maximum magnetic field of 50 kG and the focusing limit of $K_f=160$ which is a design feature of the magnet determined by the hill-valley flutter field and the spiraling of the sectors. So the maximum kinetic energy (in MeV/u) is limited either by $(E/A) = K_b(Q/A)^2$ or by $(E/A)=K_f(Q/A)$. The optimum isochronous field is produced by a pair of superconducting coils (main coils), the iron core and 14 trim coils. The superconducting cyclotron has mainly two beam probes.

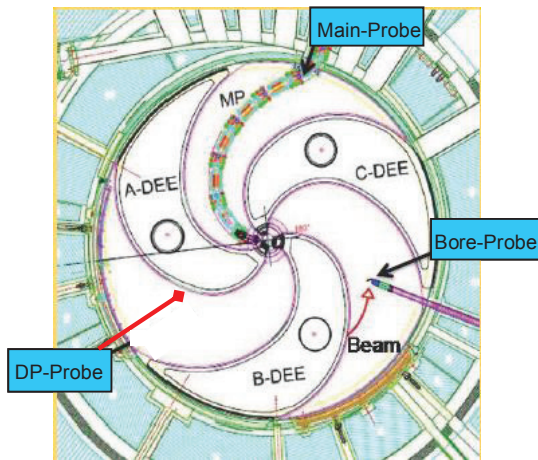


Figure 1: Schematic of the three probe locations.

[#]jdebnath@vecc.gov.in

One ‘main-probe’ (MP) running along the spiral central line of a hill. Another ‘bore scope probe’, running straight across another hill, is sometimes used as a second beam current measuring probe. One of the extraction element ports was used temporarily for installing the third beam current measuring device, which we call the ‘deflector probe’ (DP). With these three probes and the beam shadowing technique, beam off-centring were quantified at different radii.

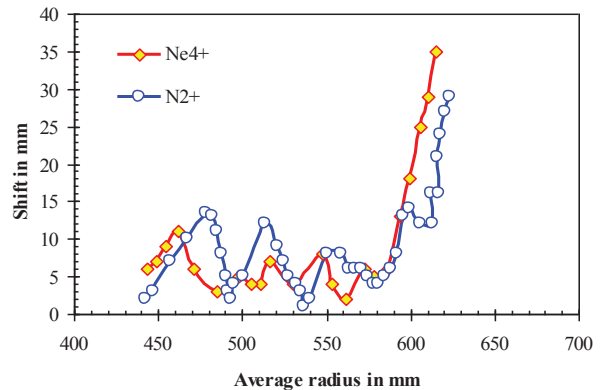


Figure 2: Beam off-centering as a function of R_{av} .

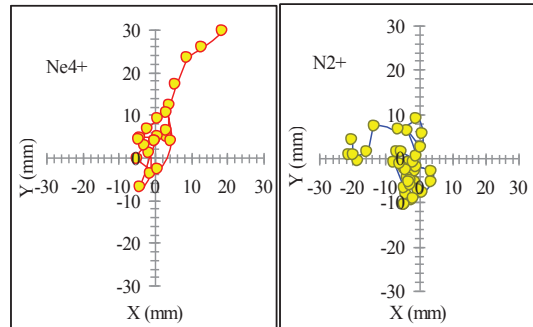


Figure 3: Locus of the Beam-centre for Ne^{4+} , $h=2$, $v_{RF}=19MHz$ and N^{2+} , $h=2$, $v_{RF}=14MHz$ beam.

Ne^{4+} beam in 2nd harmonic RF mode ($v_{RF}=19MHz$) has been accelerated up to the maximum radius but we could not extract it. We have tried to measure the beam off-centering and beam phase to understand the problem. It was observed that the coherent oscillation amplitude of the beam is ~ 5 mm up to radius ~ 580 mm. Beyond that radius, the beam continuously shifts in one direction as shown in Fig. 2 and as a result of large off-centering it is lost before reaching the deflector entry. Figure3 shows the locus of the beam centre as a function of radius obtained by beam shadowing experiment. From the beam shadowing measurements one can calculate the average

radius of the orbits as a function of radius. It is observed that due to continuous shift of the orbit centre beyond 600 mm radius the orbit size does not increase properly beyond ~650 mm. It may be noted that the deflector entry is located at 670 mm radius.

SIMUALTIONS

A field fitting code (TCFit) is used to obtain the main coil and trim coil current settings for running the cyclotron to accelerate the beam to its desired final energy fitting the given energy vs. $\text{Sin}(\phi)$ curve. It also generates the isochronous field for the other orbit-calculation codes. we use the following beam for the simulation: Ne4+, Q/A=0.20009, E=8.24MeV/u, harmonic mode h=2, ν_{RF} =19.00 MHz, B_0 =30.917 kG, V_{Dec} =40 kV, R_{Def} =668 mm. Figure4 shows the magnetic field profile obtained from 'TCFit' after fitting the phase history shown in the figure.

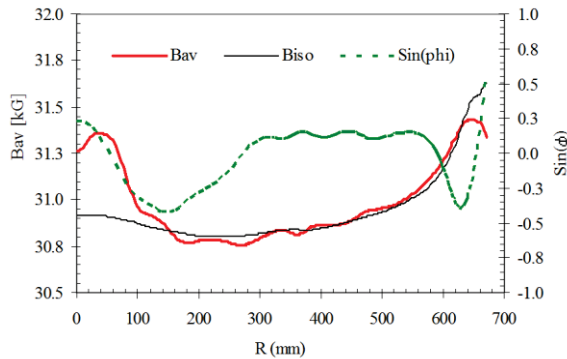


Figure 4: Average magnetic field profile and the energy vs. $\text{Sin}(\phi)$ curve for the Ne4+ beam used in simulation.

The radial profile of the betatron frequencies is shown in Fig. 5. It is seen from the graph that the beam crosses the linear resonance $\nu_r=1$ near 600 mm. The extraction radius is 667 mm. The tune diagram as shown in Fig. 6 shows the different resonance crossing as the beam reaches the final radius.

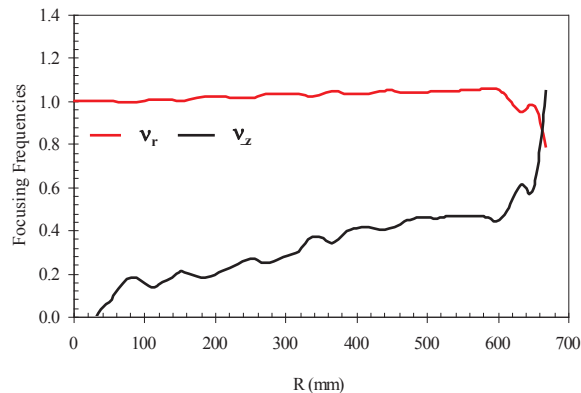


Figure 5: Radial profile of the betatron frequencies.

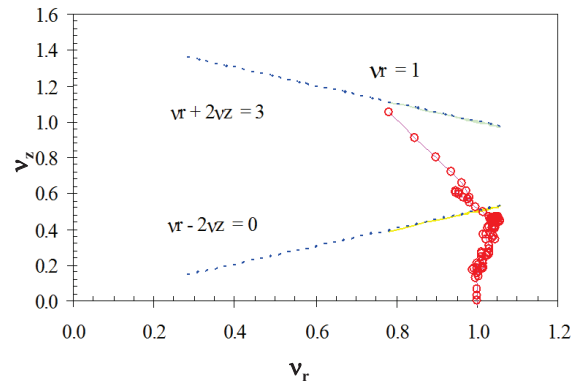


Figure 6: Tune diagram showing different resonances for the Ne4+ beam.

With the optimum field obtained from TCFit, the beam is tracked integrating the equations of motion with a code SPRGAP [2], which is an accelerated-orbit program used to study the behaviour of the beam especially in the last hundred turns before extraction, using zero width acceleration gap.

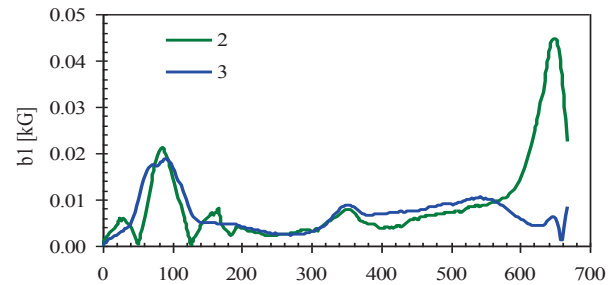


Figure 7: 1st harmonic field profiles.

We have used different 1st harmonic field profile to see the effect on the beam as it crosses the $\nu_r=1$ resonance before reaching the extraction radius. In Fig. 7 two 1st harmonic field profiles have been shown. We have remapped the magnetic field, opening the machine. Curve (2) is the b1 profile which we got just after opening the machine. Curve (3) is the b1 profile after shimming correction done in June 2013.

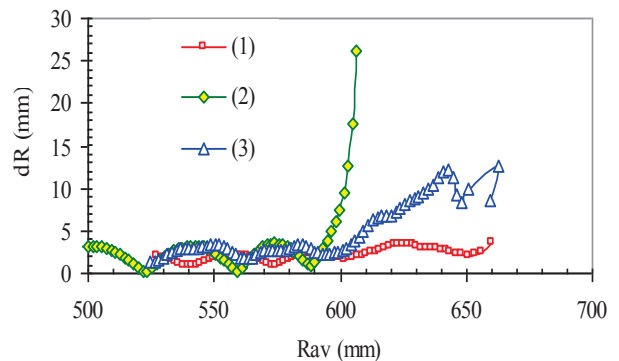


Figure 8: Beam centre shift as a function average radius.

From the beam tracking it is found as can be seen from the R-Pr diagram (Fig. 9) that with large 1st harmonic gradient the beam is not reaching the deflector entry (667 mm, 336°).

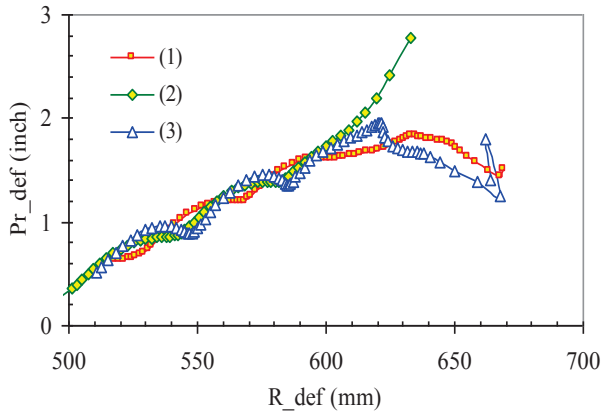


Figure 9: R-Pr values taken at each turn as the beam crosses an angle 336° (deflector entry).

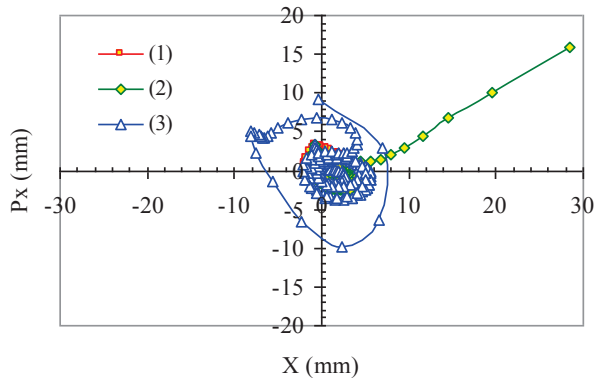


Figure 10: x-px diagram for different b1 profile.

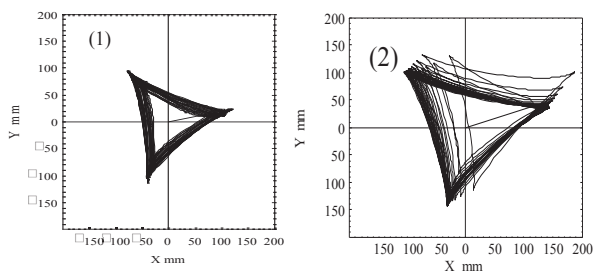


Figure 11: Locus of the instantaneous centre of curvature for case (1) and (2).

It is found from the simulation that the 1st harmonic field as shown in curve (2) is shifting the beam in one direction after crossing the resonance, not allowing it to precess around the machine centre. As a result of the large 1st harmonic field gradient around 600 mm, the beam was not reaching the deflector entry with proper path. The x-P_x diagram also shows the effect of large 1st harmonic field gradient effect. The Radial displacement and conjugate momentum are defined as:

$$x = R - R_{eo} \quad P_x = P_r - P_{r_{eo}}$$

R_{eo} is the equilibrium orbit radius at a given energy. R is the radius of the accelerated equilibrium orbit. Here the (x, p_x) points give the deviation from the equilibrium orbit at each energy. These (x, p_x) values provide direct information on the radial oscillations being performed by the accelerated orbit. We have plotted $x \sim p_x$ once per revolution when the beam crosses the sector centre.

We have studied the effect of 2nd harmonic field as shown in figures with the code SPRGAP. When there is a large gradient around $v_r=1$ crossing zone, then the beam is shifting in a direction producing large off-centering and as a result of the large off-centering the beam is getting lost hitting the wall.

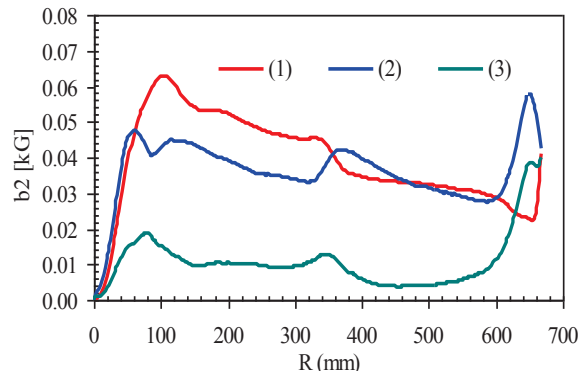


Figure 12: 2nd harmonic field profiles.

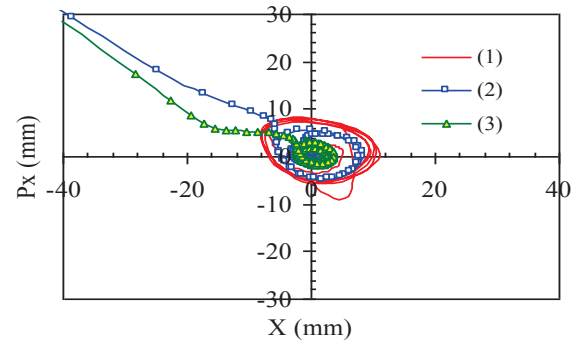


Figure 13: x-px diagram in case b2 profile.

CONCLUSION

The magnetic field has been mapped again; corrections have been done to minimize the 1st harmonic field with the constraints that many components are kept intact so that we can go for beam trial very quickly.

REFERENCES

- [1] C. Mallik, *et al.*, “First Beam Acceleration in Kolkata Superconducting Cyclotron and its Present Status”, CYCLOTRONS 2010.
- [2] M.M. Gordon *et al.*, “Effect of Spiral Electric Gaps in Superconducting Cyclotrons”, NIM 169 (1980).